Moment Induced by Liquid Payload During Spin-up Without a Critical Layer

Charles H. Murphy*
U.S. Army Ballistic Research Laboratory, Aberdeen Proving Ground, Maryland

For a fully spun-up liquid payload, eigenfrequencies and liquid side moments induced by projectile coning motion have been computed by a linear boundary-layer theory. For partially spun-up liquids, this theory can fail due to the presence of a critical layer in which the local angular velocity of the spinning motion is near the angular velocity of the projectile's coning motion. Late in the spin-up process, when more than 90% of the spin angular momentum has been acquired by the liquid, a critical layer usually does not exist. In this paper, a linear boundary-layer theory is developed to predict eigenfrequencies and the liquid moment during late spin-up times. The predicted eigenfrequencies agree well with those computed by the linearized Navier-Stokes technique of Gerber and Sedney. The side moments predicted by the linear boundary-layer theory are available to projectile designers for flight stability analysis.

Nomenclature

a	= radius of a liquid-filled cylindrical cavity
c	= one-half the length of the liquid-filled cylindrical cavity
I	= liquid angular momentum ratio, Eq. (7)
$\hat{K}$	$= K_{10}\exp(i\phi_{10})$
K_{10}	= magnitude of the coning motion
k_l	$= \kappa(a/c)Re^{-1/2}$
k_t	$= 0.035(a/c)Re^{-1/5}$
m_L	= mass of liquid
p	= liquid pressure
p_s	= liquid pressure perturbation
$r,\tilde{r}$	= radial coordinates in inertial and aeroballistic systems, respectively
r_f	= the front: the r value separating the rotating and nonrotating fluids
Re	= Reynolds number, $a^2\dot{\phi}/\nu$
s	$= (\epsilon + i)\tau$
t	= time
u_s, v_s, w_s	= components of liquid velocity perturbation in the inertial system
V_x, V_r, V_θ	= velocity components of the liquid in the inertial cylindrical system
$\hat{w}$	$= V_\theta(r\dot{\phi})^{-1}$
$\hat{w}_a$	= average value of $\hat{w}$, Eq. (21)
$x,\tilde{x}$	= axial coordinates in inertial and aeroballistic systems, respectively
$\tilde{\alpha},\tilde{\beta}$	= angles of attack and sideslip, respectively, in the aeroballistic system
κ	= parameter in k_ℓ, usually 0.5
ϵ	= exponential damping per cycle of coning motion
$\theta,\tilde{\theta}$	= azimuthal coordinates in inertial and aeroballistic systems, respectively
ν	= kinematic viscosity
ρ_L	= liquid density
τ	= nondimensional frequency of the coning motion
τ_{kn}	= eigenvalue of τ
ϕ	= spin angle, $\dot{\phi}t$
ϕ_{10}	= orientation angle of $\hat{K}$
$\dot{\phi}$	= spin rate

Presented as Paper 84-0229 at the AIAA 22nd Aerospace Sciences Meeting, Reno, Nev., Jan. 9-12, 1984; submitted Feb. 29, 1984; revision submitted July 31, 1984. This paper is declared a work of the U.S. Government and therefore is in the public domain.

*Chief, Launch and Flight Division. Fellow AIAA.

Introduction

THE prediction of the complete moment exerted by a spinning liquid payload on a spinning projectile performing a pitching and yawing motion has been a problem of considerable interest to the Army for some time. For a fully spinning inviscid liquid, the linear side moment was first computed by Stewartson[1] by use of eigenfrequencies determined by the fineness ratio of the cylindrical container. Wedemeyer[2] introduced boundary layers on the walls of the container and was able to determine viscous corrections for Stewartson's eigenfrequencies, which could then be used in Stewartson's side moment calculation. Murphy[3] then completed the linear boundary-layer theory by including all pressure and wall shear contributions to the liquid-induced side moment. The Stewartson-Wedemeyer eigenvalue calculations have been improved for low Reynolds numbers by Kitchens et al.[4] through the replacement of the cylindrical wall boundary approximation by a linearized Navier-Stokes approach. Next, Gerber et al.[5,6] extended this linearized Navier-Stokes technique to compute better side moment coefficients for Reynolds numbers less than 10,000. Finally, the roll moment for a fully spun-up liquid was computed by Murphy.[7]

Since liquid payloads can require as much as half the flight time to reach full spin-up,[8] considerable theoretical effort has been expended on predicting the spin-up process and its effect on the liquid-induced moment. Wedemeyer[9] developed a very simple model of the spin-up process, which has been extended by other authors.[10-12] The calculation of eigenvalues and side moment during spin-up is, however, a difficult task. Karpov[13] made use of a suggestion by Wedemeyer to obtain an approximation for the liquid side moment. Reddi[14] attempted to solve the inviscid perturbation equations but had considerable difficulty with a singular critical layer which is usually present. A critique of this work is given by Lynn[15] who did get a solution for axisymmetric waves for which no critical layer is present. Sedney and Gerber[16] extended their linearized Navier Stokes perturbation to calculate spin-up eigenfrequencies in the presence of a critical layer.

Although Sedney and Gerber have been able to overcome the mathematical difficulties associated with the singular critical layer, their method requires the solution of six complicated first-order differential equations. This critical layer occurs in an annular region in which the angular velocity of the liquid spinning motion is near one of the two angular frequencies of the projectile's transverse motion. Fortunately, late in the spin-up process the critical layer does not usually ex-

ist, and the simple linear boundary-layer theory can be successfully extended to predict late spin-up eigenfrequencies and liquid side moment. As we shall see, this approach involves the solution of only one second-order differential equation.

Herein this theory will be derived for a liquid near full spin-up and validity bounds in terms of flight time will be determined. Eigenfrequencies computed by this basically inviscid theory are shown to compare very well with those computed by the Gerber-Sedney linearized Navier-Stokes theory. Finally, side moment calculations are made to show the significant changes that occur during this late spin-up period.

Basic Equations

A fully filled cylindrical cavity with radius a and height $2c$ will be considered. According to Wedemeyer,[9] the spin-up flow is driven by Ekman-layer flows at the flat end walls. These Ekman layers draw fluid in near the axis, impart rotation to it, and eject it near the cylindrical wall. The flow exterior to these Ekman layers on the end walls and a boundary layer on the cylindrical lateral walls can be approximated by a two-dimensional rotating flow with circumferential velocity V_θ. A projectile attains full spin during 10-12 ms of motion down a gun barrel. If the spin is assumed to grow from an impulsive start at zero spin to a constant value of $\dot{\phi}$, the resulting circumferential velocity has the form

$$V_\theta = r\dot{\phi}\hat{w}(r,\phi) \tag{1}$$

where $\phi = \dot{\phi}t$. The boundary conditions for $\hat{w}$ are: (The proper numerical way to treat these discontinuous conditions is given in Ref. 17.)

$$\hat{w}(r,0) = 0 \qquad 0 \le r < a \tag{2}$$

$$\hat{w}(a,\phi) = 1 \qquad \phi > 0 \tag{3}$$

$$\frac{\partial \hat{w}(0,\phi)}{\partial r} = 0 \qquad \phi > 0 \tag{4}$$

Wedemeyer derived a partial differential equation for $\hat{w}(r,\phi)$ which was numerically integrated by Sedney and Gerber.[12] The equation has the following form:

$$\frac{\partial \hat{w}}{\partial \phi} + \hat{V}\left[2\hat{w} + r\frac{\partial \hat{w}}{\partial r}\right] = \frac{a^2}{Re}\left[\frac{\partial^2 \hat{w}}{\partial r^2} + \frac{3}{r}\left(\frac{\partial \hat{w}}{\partial r}\right)\right] \tag{5}$$

where

$$\hat{V} = -k_\ell(1-\hat{w}) \qquad \text{laminar Ekman layers}$$

$$= -k_t(1-\hat{w})^{8/5}(r/a)^{3/5} \qquad \text{turbulent Ekman layers}$$

and k_ℓ and k_t are defined in the Nomenclature. Wedemeyer derived a very simple laminar Ekman-layer solution that has a discontinuity in shear at an interior point.

$$\hat{w} = 0 \qquad r \le r_f$$

$$= \frac{1-(r_f/r)^2}{1-(r_f/a)^2} \qquad r_f \le r \le a \tag{6}$$

where

$$r_f = ae^{-k_\ell \phi}$$

According to this solution, the flowfield is divided into two regions: an inner core flow that is stationary and an outer rotating flow. The boundary $r = r_f$ is an inward-moving front where the velocity has discontinuous derivatives. A numerical solution to Eq. (5), of course, does not have this discontinuity. r_f, however, is a useful measure of the extent of the spin-up process. Laminar Ekman-layer flow solutions of Eq. (5) have been computed for $Re = 40{,}000$, $c/a = 4.0$, and are compared for an early time, $\phi = 800$ rad ($r_f = 0.6$), in Fig. 1, and for a late time, $\phi = 2600$ rad ($r_f = 0.2$), in Fig. 2. The extent of spin-up can be described by the ratio of the liquid angular momentum to the fully spun-up liquid angular momentum:

$$I = \frac{4}{a^4}\int_0^a r^3 \hat{w}\,dr \tag{7}$$

In Fig. 3, I is plotted vs $\phi/\sqrt{Re}$ for several conditions. Note that for larger Reynolds numbers, spin-up requires many more revolutions; i.e., much more flight time. For $\dot{\phi} = 1000\ s^{-1}$, the liquid angular momentum is 95% of that of a rigid body in 1.8 s for laminar Ekman layers ($Re = 40{,}000$) and in 9 s for turbulent Ekman layers ($Re = 10^6$).

It is now assumed that velocity components and pressure can be expressed in a more general form than used in Ref. 3.

$$V_x = R\{u_s e^{s\phi - i\theta}\}(a\dot{\phi}) \tag{8}$$

$$V_r = R\{v_s e^{s\phi - i\theta}\}(a\dot{\phi}) \tag{9}$$

$$V_\theta = r\dot{\phi}\hat{w} + R\{w_s e^{s\phi - i\theta}\}(a\dot{\phi}) \tag{10}$$

$$p = \rho_L a^2 \dot{\phi}^2 \hat{P} + R\{p_s e^{s\phi - i\theta}\}(\rho_L a^2 \dot{\phi}^2) \tag{11}$$

where

$$\hat{p} = a^{-2}\int_0^r [\hat{w}(r_1)]^2 r_1 dr_1 \tag{12}$$

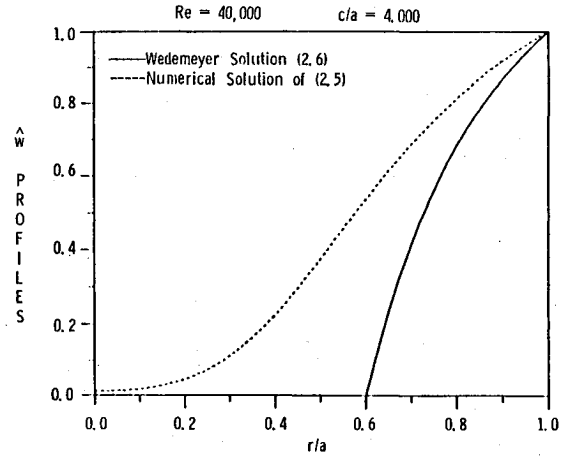

Fig. 1 Laminar flow solutions of Eq. (5) for $Re = 40{,}000$, $c/a = 4$, and $\phi = 800$ rad.

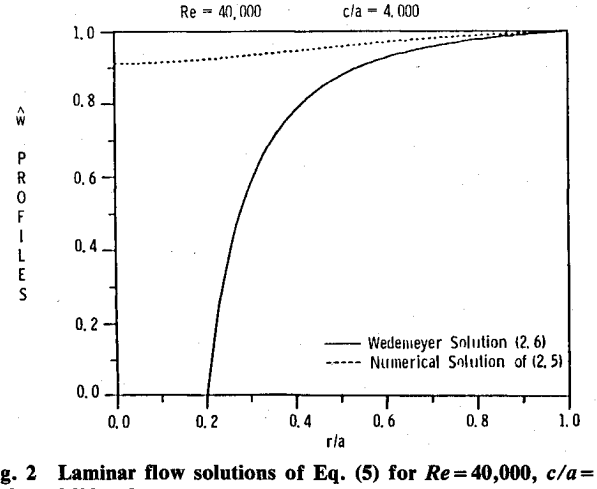

Fig. 2 Laminar flow solutions of Eq. (5) for $Re = 40{,}000$, $c/a = 4$, and $\phi = 2600$ rad.

and $R\{\ \}$ is the real part of $\{\ \}$. The basic flow, $\hat{w}(r,\phi)$, is a function of time ($\phi=\dot{\phi}t$); the perturbation theory will be valid when its variation with time is small during a period of coning motion.

Next, it is assumed that the perturbation variables u_s, v_s, w_s, and p_s are not affected by the Ekman and Stewartson layers and must satisfy the boundary conditions independently by means of their own boundary layers. This assumption is clearly somewhat arbitary but allows a first estimate of the effect of spin-up flow on the coning motion. This will be refined in the future as our understanding of the fluid mechanics improves.

The angular general motion of a spinning projectile is an epicylic motion which is the sum of two coning motions. Since the theory of this paper is linear, the response of the liquid to the combined motion is the sum of its responses to each individual coning motion. Therefore, the payload is assumed to be in coning motion defined by

$$\tilde{\beta}+i\tilde{\alpha}=\hat{K}e^{s\phi} \tag{13}$$

where

$$\hat{K}=K_{10}e^{i\phi_{10}}; \qquad s=(\epsilon+i)\tau$$

Since (x,r,θ) are cylindrical coordinates in an inertia nonconing axis system, it is convenient to introduce cylindrical coordinates $(\tilde{x},\tilde{r},\tilde{\theta})$ in an aeroballistic axis system that cones with the projectile. In the aeroballistic coordinates the walls of a cylindrical container whose center is at the projectile's center of mass have the simple coordinates $\tilde{r}=a$ and $\tilde{x}=\pm c$. At these surfaces the liquid velocity components must equal the wall velocity components:

$$u_s=(s-i)(\tilde{r}/a)\hat{K}$$

$$v_s=-(s-i)(\tilde{x}/a)\hat{K}$$

$$w_s=\left[\hat{w}(\tilde{r})+is+\tilde{r}\frac{\partial\hat{w}(\tilde{r})}{\partial r}\right](\tilde{x}/a)\hat{K} \tag{14}$$

As was done in Ref. 3, the perturbation variables are separated into inviscid and viscous components where the viscous components are solved by boundary-layer approximations:

$$u_s=u_{si}+u_{sv}, \qquad w_s=w_{si}+w_{sv}$$

$$v_s=v_{si}+v_{sv}, \qquad p_s=p_{si}+p_{sv} \tag{15}$$

For the fully spun-up liquid, the boundary-layer analysis leads to the following boundary conditions for the inviscid flow:

$$\left[v_{si}-a\delta_a\frac{\partial v_{si}}{\partial r}\right]_{r=a}=(i-s)(x/a)\hat{K} \tag{16}$$

$$\left[u_{si}\mp c\delta_c\frac{\partial u_{si}}{\partial x}\right]_{x=\pm c}=(s-i)(r/a)\hat{K} \tag{17}$$

where

$$\delta_a=\frac{1+i}{\sqrt{2(1+is)}}Re^{-1/2} \tag{18}$$

$$\delta_c=-\frac{(a/2c)(1+i)(2Re)^{-1/2}}{(1+is)}\left[\frac{1-is}{\sqrt{3+is}}+\frac{(3+is)i}{\sqrt{1-is}}\right] \tag{19}$$

δ_a and δ_c are complex parameters whose real parts act like displacement thicknesses, as can be seen from Eqs. (16) and (17). Their imaginary parts indicate time lags in the fluid response to the periodic wall motion.

During spin-up, the lateral wall boundary layer has a constant Reynolds number and is essentially unaffected, but the end wall boundary layer has an exterior flow of $r\hat{w}\dot{\phi}$ rather than $r\dot{\phi}$. As a crude approximation it will be assumed that Eq. (16) still applies during spin-up and the Reynolds number in Eq. (17) should be modified by an average $\hat{w}$.

$$\left[u_{si}\mp(\hat{w}_a)^{-1/2}c\delta_c\frac{\partial u_{si}}{\partial x}\right]_{x=\pm c}=(s-i)(r/a)\hat{K} \tag{20}$$

where

$$\hat{w}_a=\frac{2}{a^2}\int_0^a\hat{w}r\,dr \tag{21}$$

The inviscid velocity components satisfy the linearized Navier-Stokes equation for an infinite Reynolds number.

$$u_{si}=-a(s-\hat{w}i)^{-1}\frac{\partial p_{si}}{\partial x} \tag{22}$$

$$v_{si}=\left[2i(a/r)\hat{w}p_{si}-(s-\hat{w}i)a\frac{\partial p_{si}}{\partial r}\right]D^{-1} \tag{23}$$

$$w_{si}=\left[i(a/r)(s-\hat{w}i)p_{si}+\left(2\hat{w}+r\frac{\partial\hat{w}}{\partial r}\right)a\frac{\partial p_{si}}{\partial r}\right]D^{-1} \tag{24}$$

where

$$D=s^2-2\hat{w}si+3\hat{w}^2+r\frac{\partial(\hat{w}^2)}{\partial r} \tag{25}$$

Equations (22-24) now can be substituted in the continuity equation to yield a differential equation for p_{si}.

$$\frac{\partial^2 p_{si}}{\partial r^2}+r^{-1}\left[1-r\frac{\partial D}{\partial r}D^{-1}\right]\frac{\partial p_{si}}{\partial r}$$

$$-r^{-2}\left[1+2ri(s-\hat{w}i)^{-1}D\frac{\partial(\hat{w}/D)}{\partial r}\right]p_{si}=-(s-\hat{w}i)^{-2}D\frac{\partial^2 p_{si}}{\partial x^2} \tag{26}$$

Equation (26) has a strong singularity for constant-amplitude coning motion when

$$\tau=\hat{w}(r,\phi) \tag{27}$$

According to Eq. (27), the critical layer is located where the liquid angular velocity is τ and an internal resonance occurs. For an inviscid calculation, very large perturbation functions result and the much more complete linearized Navier-Stokes method is necessary. For any fixed time, the minimum value of $\hat{w}$ is its value at $r=0$; i.e., $\hat{w}_0=\hat{w}(0,\phi)$. For a portion of the

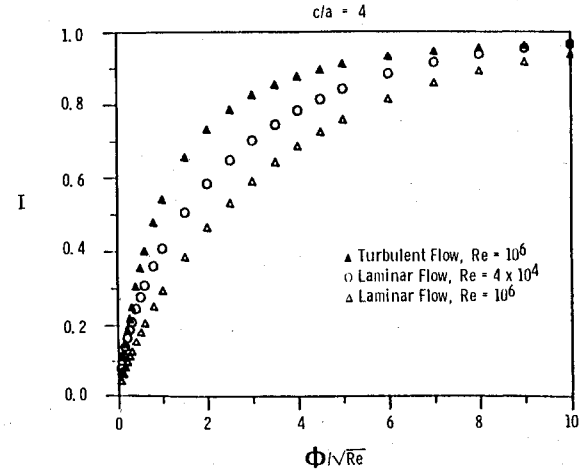

Fig. 3 Liquid angular momentum ratio vs $\phi/\sqrt{Re}$ for $c/a=4$.

spin-up period, $\hat{w}_0$ is zero and then grows to unity, which indicates a fully spun-up condition. In Fig. 4, spin angles for which $\hat{w}_0$ is 0.11 are plotted vs Reynolds number. Since projectile coning frequencies are usually less than 0.10, this figure allows estimates to be made for the region of validity of the theory of this paper. For example, at a Reynolds number of 40,000, critical layers should not exist at projectile coning frequencies for spin angles greater than 1200 rad. For a spin rate of 1000 rad/s, this means that the theory of this report should apply after 1.2 s of flight.

The solution to Eq. (26) has the form[18]

$$p_{si} = -(c/a)\left[(B_0 x/c)R_{e0}(r) + \sum_{k=1}^{N_\ell} d_{\ell k} R_{\ell k}(r)\sin(\lambda_{\ell k} x/c) + \sum_{k=1}^{N_e} d_{ek} R_{ek}(r)\sin(\lambda_{ek} x/c)\right] \tag{28}$$

where R_{e0}, $R_{\ell k}$, and R_{ek} are solutions of the following differential equation with λ equal to 0, $\lambda_{\ell k}$, and λ_{ek}, respectively:

$$R'' + r^{-1}\left[1 - r\frac{\partial D}{\partial r}D^{-1}\right]R' - r^{-2}\left[1 - r^2 c^{-2}\hat{\lambda}^2 + 2ri(s-\hat{w}i)^{-1}D\frac{\partial(\hat{w}/D)}{\partial r}\right]R = 0 \tag{29}$$

where

$$\hat{\lambda}^2 = -(s-\hat{w}i)^{-2}D\lambda^2$$

$$R(0)=0, \quad R(a)=1 \quad \text{for } \lambda = 0$$

$$=0, \quad aR'(0)=1 \quad \text{otherwise}$$

$\lambda_{\ell k}$ is selected so that

$$\left[u_{si} \mp (\hat{w}_a)^{-1/2} c\delta_c \frac{\partial u_{si}}{\partial x}\right]_{x=\pm c} = 0 \tag{30}$$

and λ_{ek} is selected so that

$$\left[v_{si} - a\delta_a \frac{\partial v_{si}}{\partial r}\right]_{r=a} = 0 \tag{31}$$

Finally, B_0 and the d_{ek}'s are selected to satisfy the endwall boundary condition [(Eq. 20)] by a least-squares fit and the $d_{\ell k}$'s are selected to satisfy the lateral boundary condition [Eq. (16)] by a similar least-squares fit.[18] When $s=(\epsilon+i)\tau$ is selected so that $d_{\ell k}$ or d_{ek} is infinite, s is an eigenvalue and its imaginary part is an eigenfrequency, τ_{kn}. (For fixed k, τ_{kl} is the smallest τ_{kn} and $\tau_{\beta n}$ increases with increasing n.)

For the fully spun-up case, Eq. (28) takes on a much simpler form since $d_{ek}=0$, $B_0=1$, $R_{e0}=r/a$, and $\lambda_{\ell k}=k(\pi/2)[1+\delta_c]$; k is an odd integer.

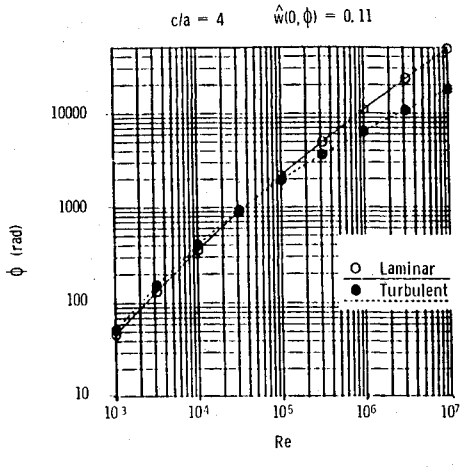

Fig. 4 Spin angles for which $\hat{w}_0 = 0.11$ vs Reynolds number, $c/a = 4$.

Liquid Moment

The linear liquid moment in response to the coning motion described by Eq. (13) can be expressed in the following form in terms of the nonspinning aeroballistic axis system, $\tilde{X}, \tilde{Y}, \tilde{Z}$, which pitches and yaws with the missile.

$$M_{L\tilde{Y}} + iM_{L\tilde{Z}} = m_L a^2 \dot{\phi}^2 \tau (C_{\mathrm{LSM}} + iC_{\mathrm{LIM}})\hat{K}e^{s\phi} \tag{32}$$

The imaginary part of the dimensionless moment coefficient C_{LIM} causes a rotation in the plane of the coning moment and is called the liquid in-plane moment coefficient while the real part C_{LSM} causes a rotation out of this plane and is called the liquid side moment coefficient. Since C_{LSM} affects the damping of the coning motion, and C_{LIM} affects only the frequency, prediction of C_{LSM} is the primary objective of any theory. The major components of the liquid moment are due to the pressure on the lateral and end walls of the container. Lesser components are due to the viscous wall shear on the lateral and end walls; thus, the liquid moment coefficient can be given as the sum of the following four terms:

$$\tau(C_{\mathrm{LSM}} + iC_{\mathrm{LIM}}) = m_{p\ell} + m_{pe} + m_{v\ell} + m_{ve} \tag{33}$$

The pressure as given by Eq. (11) is specified as a function of r and x. A linear approximation for pressure as a function of $\tilde{r}$ and $\tilde{x}$ is

$$p(p_L \dot{\phi} a^2)^{-1} = \hat{p}(\tilde{r}) + \frac{d\hat{p}}{dr}(r-\tilde{r}) + R\{p_s e^{s\phi - i\theta}\}$$

$$= \hat{p}(\tilde{r}) + R\left\{\left[p_s - \frac{\tilde{x}\tilde{r}\hat{w}^2}{a^2}\hat{K}\right]e^{s\phi - i\theta}\right\} \tag{34}$$

The pressure moments relative to the center of the cylinder are

$$\therefore m_{p\ell} = i(2\pi ac\hat{K})^{-1}e^{-s\phi}\int_{-c}^{c}\int_{0}^{2\pi}\tilde{x}e^{i\tilde{\theta}}R\{[p_s - (\tilde{x}/a)\tilde{K}]e^{s\phi - i\theta}\}\,dx\,d\theta = i(2ac)^{-1}\int_{-c}^{c} x[p_s(a,\tilde{x})\tilde{K}^{-1} - (\tilde{x}/a)]\,d\tilde{x} \tag{35}$$

$$m_{pe} = -i(a^2 c)^{-1}\int_0^a [p_s(\tilde{r},c)\hat{K}^{-1} - \tilde{r}\hat{w}^2(c/a^2)]\tilde{r}^2\,dr \tag{36}$$

Table 1 Comparison of Navier-Stokes and linear boundary-layer eigenvalues for $k=1$, $c/a=0.600$, and $\kappa=0.443$

	τ		ϵ	
r_f/a	NS	LBL	NS	LBL
	a) $Re=30{,}000$,		$n=1$	
0.300	−0.3359	−0.3355	0.012	0.010
0.235	−0.3707	−0.3681	0.010	0.008
0.026	−0.4278	−0.4282	0.007	0.006
	b) $Re=50{,}000$,		$n=2$	
0.271	0.1526	0.1540	−0.021	−0.00005
0.202	0.1648	0.1642	−0.018	−0.012
0.013	0.1745	0.1745	−0.019	−0.014

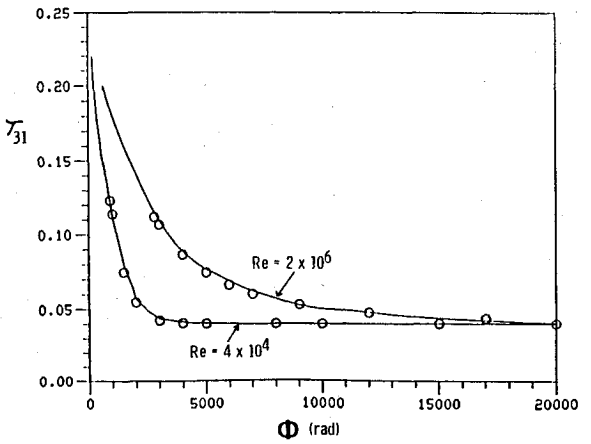

Fig. 5 Eigenfrequency τ_{31} vs spin angle ϕ for $Re=40{,}000$, $c/a=3.12$, $k=3$, $n=1$, and $\kappa=0.443$. The curves are for Sedney-Gerber NS theory (Fig. 5, Ref. 16), the circles are from linear boundary-layer theory.

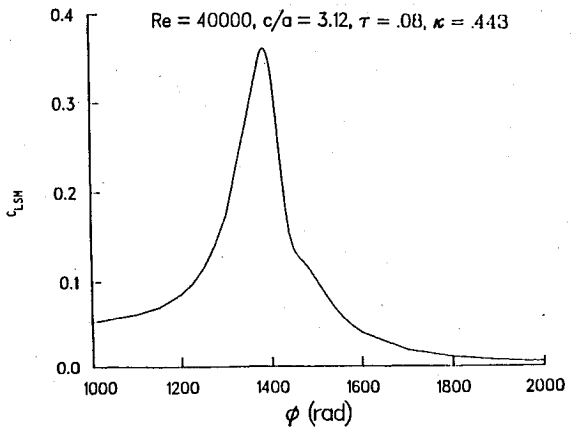

Fig. 6 Liquid side moment coefficient C_{LSM} vs spin angle for $\tau=0.08$ and the conditions of Fig. 5.

The viscous components of the liquid moment are computed by the formula of Eqs. (7.2) and (7.3) of Ref. 3 by using the new bounday condition for w_s as given by Eq. (14) and replacing Re by $\hat{w}_a Re$ in the endwall boundary-layer profiles.

Numerical Calculations

In Ref. 16, Navier-Stokes calculations of eigenfrequencies are given for $Re=5000$, 30,000, 40,000, 50,000 and 2×10^6. δ_c was taken to be zero, and laminar Ekman layers were assumed for all cases except $Re=2\times10^6$, which involved turbulent Ekman layers. The degree of spin-up is indicated by r_f/a as defined in Eq. (6). This parameter varies from 1 to 0 as time varies from 0 to ∞ (fully spun-up).

Table 1 compares the Navier-Stokes (NS) perturbation values of τ and ϵ with the linearized boundary-layer (LBL) theory values. In the first part of this table, the eigenfrequencies for $n=1$ are negative and, hence, no critical layer exists. The frequencies agree well although the comparison of the damping rates is much poorer. In the second part of the table, for $n=2$, a critical layer does exist for $r_f/a=0.27$ ($\hat{w}=0.02$) but the nonzero value of ϵ seems to be sufficient to allow a good evaluation of τ. The very small value of ϵ does indicate the nearness of an instability. The NS value of damping in the presence of a critical layer is a healthy value and shows the power of this method in the presence of a critical layer.

In Fig. 5, the eigenfrequencies are compared for both laminar and turbulent Ekman layers; and agreement is good for later spin-up. The Navier-Stokes values are, of course, the

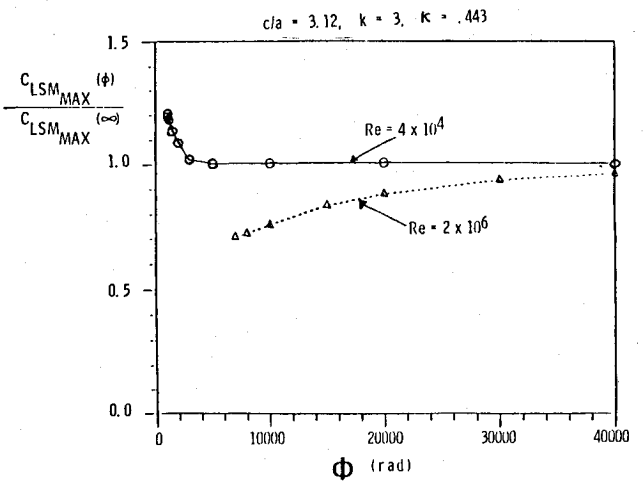

Fig. 7 Ratio of maximum side moment coefficients vs roll angle ϕ for $Re=4\times10^4$, 2×10^6, $c/a=3.12$, $k=3$, and $n=1$.

only ones appropriate for early spin-up. The LBL theory is, however, the first to compute moment coefficients during spin-up. This is not an intrinsic limitation of the NS theory and approximate numerical codes are presently being developed for the Navier-Stokes theory.[19] An example of the variation of the side moment coefficient with time is shown in Fig. 6 for the conditions of the laminar curve of Fig. 5. For the fixed coning frequency of 0.08, the side moment coefficient is computed for ϕ ranging from 1000 to 2000 rad. This covers the region between the disappearance of the critical layer and the establishment of a steady-state spin profile. As could have been predicted from Fig. 5, the peak occurs at $\phi=1400$ rad. This, however, is the first calculation of the value of this peak side moment coefficient.

For the conditions of Fig. 6, the fully spun-up values of τ_{31} and its associated maximum C_{LSM} are 0.040 and 0.312. According to Figs. 5 and 6, at $\phi=1400$, these quantities are approximately 0.08 and 0.36. Thus, the peak side moment coefficient at this point of spin-up is 15% greater than its fully spun-up value.

In Fig. 7, we plot the ratio of this maximum side moment coefficient to its value at $\phi=\infty$ vs ϕ. For the smallest value of ϕ for which the critical layer is not present, i.e., 1000, the maximum side moment coefficient is 40% larger than its fully spun-up value. In this figure, the corresponding plot for $Re=2\times10^6$ is also given. For the higher Reynolds number, the spin-up time is much larger and is in excess of 40,000. At the disappearance of the critical layer for ϕ of 7000, the peak side moment coefficient is 30% less than its fully spun-up value.

Summary

During the later portion of the spin-up process, the period of the circumferential flow is a function of radial distance from the spin axis but is never near the period of the coning motion, i.e., no critical layer exists. For this time period, a simple linear boundary-layer theory has been developed to compute eigenfrequencies and side moment coefficients. This theory requires much less computational time than a more complete Navier-Stokes perturbation theory but yields essentially the same eigenfrequencies after the critical layer has vanished. Projectile designers are now able to compute in a routine manner side moment coefficients for over two-thirds of the spin-up process.

References

[1] Stewartson, K., "On the Stability of a Spinning Top Containing Liquid," *Journal of Fluid Mechanics*, Vol. 5, Pt. 4, Sept. 1959, pp. 577-592.

[2]Wedemeyer, E.H., "Viscous Correction to Stewartson's Stability Criterion," BRL Rept. 1325, June 1966.

[3]Murphy, C.H., "Angular Motion of a Spinning Projectile With a Viscous Liquid Payload," BRL Memorandum Rept., ARBRL-MR-03194, Aug. 1982; also, *Journal of Guidance, Control, and Dynamics,* Vol. 6, July-Aug. 1983, pp. 280-286.

[4]Kitchens, C.W. Jr., Gerber, N., and Sedney, R., "Oscillations of a Liquid in a Rotating Cylinder: Solid Body Rotation," BRL Tech. Rept., ARBRL-TR-02081, June 1978.

[5]Gerber, N., Sedney, R., and Bartos, J.M., "Pressure Moment on a Liquid-Filled Projectile: Solid Body Rotation," BRL Tech. Rept., ARBRL-TR-02422, Oct. 1982.

[6]Gerber, N. and Sedney, R., "Moment on a Liquid-Filled Spinning and Nutating Projectile: Solid Body Rotation," BRL Tech. Rept. ARBRL-TR-02470, Feb. 1983.

[7]Murphy, C.H., "Liquid Payload Roll Moment Induced by a Spinning and Coning Projectile," BRL Tech. Rept. ARBRL-TR-02521, Sept. 1983; also, AIAA Paper 83-2142, Aug. 1983.

[8]Mark, A., "Measurements of Angular Momentum Transfer in Liquid-Filled Projectiles," BRL Tech. Rept., ARBRL-TR-02029, Nov. 1977.

[9]Wedemeyer, E.H., "The Unsteady Flow Within a Spinning Cylinder," *Journal of Fluid Mechanics,* Vol. 20, Pt. 3, 1964, pp. 383-399; also, BRL Rept. 1225, Oct. 1963.

[10]Kitchens, C.W. Jr., "Ekman Compatibility Conditions in Wedemeyer Spin-Up Model," *Physics of Fluids,* Vol. 23, Pt. 5, May 1980, pp. 1062-1064.

[11]Kitchens, C.W. Jr., Gerber, N., and Sedney, R., "Spin Decay of Liquid-Filled Projectiles," *Journal of Spacecraft and Rockets,* Vol. 15, Nov.-Dec. 1978, pp. 348-354; also, BRL Rept. 1996, July 1977, and BRL Rept. 2026, Oct. 1977.

[12]Sedney, R. and Gerber, N., "Viscous Effects in the Wedemeyer Model of Spin-Up From Rest," BRL Tech. Rept., ARBRL-TR-02493, June 1983.

[13]Karpov, B.G., "Dynamics of Liquid-Filled Shell: Instability During Spin-Up," BRL Memo. Rept. 1629, Jan. 1965.

[14]Reddi, M.M., "On the Eigenvalues of Couette Flow in a Fully-Filled Cylindrical Container," Franklin Institute Research Laboratory, Philadelphia, Pa., Rept. F-B2294, 1967.

[15]Lynn, Y.M., "Free Oscillations of a Liquid During Spin-Up," BRL Rept. 1663, Aug. 1973.

[16]Sedney, R. and Gerber, N., "Oscillations of a Liquid in a Rotating Cylinder: Part II, Spin-Up," BRL Tech. Rept., ARBRL-TR-02489, May 1983.

[17]Sedney, R., and Gerber, N., "Treatment of the Discontinuity in the Spin-Up Problem with Impulsive Start," BRL Tech. Rept., ARBRL-TR-02520, Sept 1983.

[18]Murphy, C.H., "Moment Induced by Liquid Payload During Spin-Up Without a Critical Layer," BRL Tech. Rept., ARBRL-TR-02581, Aug. 1984; also, AIAA Paper 84-0229, Jan. 1984.

[19]Gerber, N.,"Contribution of Pressure to the Moment During Spin-Up on a Nutating Liquid-Filled Cylinder: Ad Hoc Model," BRL Tech. Rept., ARBRL-TR-02563, June 1984.